In Vivo Bioluminescence Imaging of Furin Activity in Breast Cancer Cells Using Bioluminogenic Substrates

ARTICLE *in* BIOCONJUGATE CHEMISTRY · AUGUST 2009

Impact Factor: 4.51 · DOI: 10.1021/bc9002508 · Source: PubMed

3 AUTHORS, INCLUDING:

Gaolin Liang
University of Science and Technology of China
66 PUBLICATIONS **2,244** CITATIONS

SEE PROFILE

Published in final edited form as:
Bioconjug Chem. 2009 August 19; 20(8): 1660–1666. doi:10.1021/bc9002508.

In vivo bioluminescence imaging of furin activity in breast cancer cells using bioluminogenic substrates

Anca Dragulescu-Andrasi, **Gaolin Liang**, and **Jianghong Rao***
Department of Radiology, Molecular Imaging Program at Stanford, Bio-X Program, and Cancer Biology Program, Stanford University School of Medicine, 1201 Welch Road, Stanford, California 94305

Abstract

Furin, a proprotein convertases family endoprotease, processes numerous physiological substrates and is overexpressed in cancer and inflammatory conditions. Non-invasive imaging of furin activity will offer a valuable tool to probe the furin function over the course of tumor growth and migration in the same animals in real time and directly assess the inhibition efficacy of drugs in vivo. Here, we report successful bioluminescence imaging of furin activity in xenografted MBA-MB-468 breast cancer tumors in mice with bioluminogenic probes. The probes are conjugates of furin substrate, a consensus amino acid motif R-X-K/R-R (X, any amino acid), with the firefly luciferase substrate D-aminoluciferin. In the presence of luciferase reporter, the probes are unable to produce bioluminescent emission without furin activation. Blocking experiments with a furin inhibitor and control experiments with a scrambled probe showed that the bioluminescence emission in the presence of firefly luciferase is furin-dependent and specific. After the furin activation, a 30-fold increase in the bioluminescent emission was observed in vitro and on average 7-8 fold contrast between the probe and control was seen in the same tumor xenografts in mice. Direct imaging of furin activity may facilitate the study of furin function in tumorigenicity and discovery of new drugs for furin-targeted cancer therapy.

Keywords

bioluminescence imaging; furin; luciferase; caged D-aminoluciferin

INTRODUCTION

In vivo bioluminescence imaging (BLI) uses luciferase enzymes (such as firefly luciferase, *Renilla* luciferase, green or red click beetle luciferase) as reporters to generate light emission during the catalytic oxidation of their substrates for non-invasive imaging of biological targets and processes in intact cells and living animals (1-3). Because of its extremely high sensitivity and relatively simple instrument setup, BLI has been extensively used as molecular imaging technique in small animals, particularly for cancer imaging research. For example, BLI is used to measure the mass and location of implanted cells in animals (4), to evaluate the efficacy of anticancer drugs (5-7), and to detect protein-protein interactions in living cancer cells (8-9).

BLI employs both the enzyme and substrate to generate the light emission, and many strategies have been developed to regulate the activity of the reporter enzyme at the various levels (transcriptional, post-transcriptional, translational, and post-translational) for

*Phone: 650-736-8563, Fax: 650-736-7925, jrao@stanford.edu

molecular imaging (10). Alternatively, the substrates may be chemically converted into an inactive “caged” form that can be activated by certain biological targets to generate the original substrates for imaging. For example, the substrates of firefly luciferase have been conjugated to caspase-3 peptide substrate and beta-lactam to produce bioluminogenic probes for imaging caspase-3 (11,12) and beta-lactamase activity (13). Herein, we report the design of luminogenic probes based on D-aminoluciferin for imaging furin activity in breast cancer cells in vivo.

Furin, one of the seven endoproteases that belong to the proprotein convertases family, is ubiquitously expressed in mammalian cells processing and activating a wide variety of proprotein substrates (14). The physiological substrates of furin include growth factors and hormones (e.g. pro-β-NGF and TGF-β), receptors such as insulin proreceptor, plasma proteins, and as well as proteases like membrane type 1-matrix metalloproteinase (MT1-MMP) and matrix metalloproteinases (15). Upregulation of furin mRNA was identified in head and neck tumors, breast tumors, and lung cancer by means of RT-PCR and in situ hybridization (16). Recent reports have indicated that furin is a target of hypoxia-inducible factor 1 (HIF-1) and that hypoxia induces elevated levels of furin leading to more aggressive tumors (17). It has been demonstrated that furin inhibition correlates with decreased invasiveness and tumorigenicity of several human cancer cells in vivo (18,19). Considering the vital role of furin in the tumor formation and invasion, the ability to image its activity in vivo will offer a valuable tool to probe the furin function over the course of tumor growth and migration in the same animals in real time and provide a means to assess in vivo inhibition efficacy of drugs. However, no probes are currently available for non-invasive imaging of furin activity in living animals.

Furin performs a calcium-dependant proteolytic cleavage at the *C*-terminus of a consensus amino acid motif R-X-K/R-R (X, any amino acid) (20). This tetrapeptide motif provides sufficient specificity to bind the active furin (21). To take advantage of the high sensitivity of BLI, we developed bioluminogenic furin probes by conjugating the furin substrate to the luciferase substrate D-aminoluciferin. Here we show that these bioluminogenic probes are specifically activated by furin and produce bioluminescence emission in the presence of firefly luciferase in vitro, in living breast cancer cells, and in breast cancer tumor xenografts in mice.

MATERIALS AND METHODS

Probe syntheses

All peptides were synthesized using standard Fmoc-protocol on a trityl chloride resin (Novabiochem). After sequence completion the peptides were cleaved from the solid support without removing the protecting groups of the amino acids (Pbf for Arg, Boc for Lys, tBu for Tyr) using 1% TFA in dichloromethane. 2-cyano-6-aminobenzothiazole (CABT) was synthesized as previously described (22). All aminoluciferin-peptide conjugates were obtained using a three-step post-synthetic protocol as described below.

First, CABT was coupled to the C-terminal carboxylic acid group using the following procedure: Ac-R(Pbf)VR(Pbf)R(Pbf)-COOH (300 mg, 0.22 mmol) was dissolved in dry THF (3 mL). N-methylmorpholine (65 μL, 0.56 mmol) and isobutyl chloroformate (32 μL, 0.27 mmol) were added. The reaction mixture was stirred at room temperature for 30 min. Afterward, CABT (60 mg, 0.34 mmol) was added and the reaction mixture was stirred at room temperature overnight. The CABT-peptide conjugate was purified by RP-HPLC and then the solvent was removed by rotary evaporation and dried.

Second, the protection groups were removed using 95% TFA, 2.5 % water and 2.5% TIPS and then the peptide was precipitated with ether, washed, dried and used for the next step without further purification.

Third, the yellow solid was dissolved in PBS (1 mL). D-cysteine hydrochloride monohydrate (38 mg, 0.22 mmol) was dissolved in water, adjusted at pH 8.5 with sodium carbonate and added to the CABT-peptide solution. The reaction mixture was further adjusted to pH 8 and stirred at room temperature for 20 min. The product, Ac-RVRR-AmLuc was purified by RP-HPLC and lyophilized to give a light-yellow foamy solid (total yield: 21%). The final identify of the products was confirmed with mass spectroscopic analyses (Supplementary Materials).

Cell culture and tumor xenografts generation

All cell culture reagents were purchased from Invitrogen unless otherwise noted. MDA-MB-468 (human breast adenocarcinoma) cells, transduced with a retrovirus (pMSCV/L2G) to express a dual reporter containing firefly luciferase (Fluc) and green fluorescent protein (GFP), were kindly supplied by Dr. Christopher Contag (Stanford University). MDA-MB-468 $Fluc^+$ cells were cultured in DMEM (high glucose, 4500 mg/L-D-glucose, 110 mg/L sodium pyruvate) supplemented with 10% fetal bovine serum (FBS) and penicillin-streptomycin (100 units/mL) at 37 °C in a humidified atmosphere 5% CO_2 incubator. To generate tumor xenografts in mice, MDA-MB-468 $Fluc^+$ cells (10×10^6) were implanted subcutaneously in the mid-dorsal region of each 4-weeks-old female nude mouse (*Nu/Nu*, Charles River). Tumors were allowed to grow for 10 days and reach sizes between 5-7 mm before imaging.

In vitro bioluminescence measurements

Probes were diluted to a final concentration of 50 μM in DPBS containing Ca^{2+} and Mg^2, and incubated for 1h at room temperature with or without 4U furin (New England BioLabs). Subsequently, 20 μL of luciferase assay buffer (Promega), and 1 μL of QuantiLum® recombinant luciferase solution (Promega), diluted to a concentration of 0.13 mg/mL in 1mg/mL BSA solution in PBS, were added. The luminescence was immediately measured using a $20/20^n$ Single Tube Luminometer (Turner BioSystems) at a 1s integration time in every 5 min. for one hour.

Cell bioluminescence imaging

MDA-MB-468 $Fluc^+$ cells were grown in 60 mm dishes to reach 80-90% confluence. After washing twice with PBS, cells were detached using a plastic cell scraper, diluted in 2 mL of PBS and counted. Next, cells were centrifuged down, dissolved in DPBS (containing Mg^{2+} and Ca^{2+}) and placed in the 96-well plate at 3×10^5 cells/well. The furin probes were added immediately before the imaging. In the inhibition experiments, 300 μM of furin inhibitor (Decanoyl-RVKR-CMK, CalBiochem) was added. Bioluminescence images were acquired every 5 min. for 2h using an optical imaging system (IVIS 200; Xenogen Corp.) at a 50 s integration time. Circular regions of interest (ROI) were drawn over each well and quantified using Living Image software (Xenogen Corp). The background of an empty well was subtracted from the total signal. The results were reported as total photon flux within an ROI in photons per second.

Fluorescence immunostaining

MDA-MB-468 $Fluc^+$ cells were plated on glass coverslips in 24-well plates at 70% confluence and fixed with 4% paraformaldehyde for 20 min next day. Subsequently, fixed cells were washed 3 times with DPBS and permeabilized with 1% Triton X-100/PBS for 20

min, followed by blocking with 1% non-fat milk solution in PBS for 20 min. at room temperature. After blocking, cells were incubated with primary antibody (1:100, anti-furin rabbit polyclonal antibody, Biomol International, diluted with 1% non-fat milk PBS solution) for 1h at 37 °C. After three times washing with PBS and once with 1% non-fat milk, cells were incubated with secondary antibody (1: 100, goat polyclonal anti-rabbit IgG rhodamine conjugate) for 30 min. at 37 °C. After washing with PBS and distilled water, the final samples were mounted on a glass slide with mounting media containing DAPI. Images were acquired using an Axiovert 200M fluorescence microscope (CarlZeiss MicroImaging, Inc., Thornwood, NY) equipped with a 63x objective. Acquisition time was 150 ms for DAPI and 600 ms for rhodamine channel, respectively. For MDA-MB-468 tumor tissue staining, tumors were sectioned at a thickness of 10 μm, placed on glass slides and fixed with acetone on ice for 10 min. The same staining protocol for fixed cells applied to them for furin imaging.

In vivo bioluminescence imaging

Animal handling was performed in accordance with Stanford UniversityAnimal Research Committee guidelines. Prior imaging, all mice bearing MDA-MB-468Fluc$^+$ subcutaneous tumors were anesthetized using isoflurane gas (2% isoflurane in oxygen, 1 L/min) during all injection and imaging procedures. Mice were imaged in a light-tight chamber using an in vivo optical imaging system (IVIS 200; Xenogen Corp.) equipped with a cooled charge-coupled device (CCD) camera. Mice were imaged 1min. after tail vein injection of 100 μL of 10 mM probe solution with an acquisition time of 1 min, and a gray-scale reference image was obtained before the acquisition of a bioluminescence image. The pseudo-colored bioluminescence images (in photons/s/cm2/steradian) were superimposed over the gray-scale photographs of the animals. Circular ROIs were drawn over the tumor areas and quantified using Living Image software version 3.0 (Xenogen Corp.). The results were reported as total photon flux within an ROI in photons per second.

RESULTS

Luminogenic probes specifically detect furin activity in vitro

D-aminoluciferin, an analogue of D-luciferin, is a bioluminescent substrate for luciferase enzyme. Derivatization of its amino group with amino acids renders D-aminoluciferin a poor substrate for luciferase with drastically decreased photon production efficiency presumably due to the steric hindrance at the active site of firefly luciferase (23). We therefore designed our bioluminogenic furin probes by coupling D-aminoluciferin to the C-terminus of furin recognition peptide sequences, such as previously reported furin substrates RVRR and RYKR (24,25), affording two bioluminogenic furin probes: Ac-RVRR-Aminoluciferin (RVRR-AmLuc) and Ac-RYKR-Aminoluciferin (RYKR-AmLuc) (Scheme 1). Because furin cleaves at the C-terminal to the last arginine residue, small molecules at this site such as 7-amino-4-methylcoumarin can be attached at this position and the resulting conjugate can still be recognized and processed by furin (26). Both probes should be a poor substrate for firefly luciferase and would produce little light emission. In the presence of furin, the probes will be hydrolyzed to remove the peptide caging group and generate free D-aminoluciferin which will subsequently produce light emission in the presence of firefly luciferase. Therefore, the activity of furin can be measured from the firefly luciferase based bioluminescence assay. As a control, we synthesized another conjugate with a scrambled amino acid sequence that should not be recognized by furin, Ac-RRKY-Aminoluciferin (RRKY-AmLuc) (Scheme 1).

First, we evaluated our probes in vitro by measuring the bioluminescent signal as a function of time in the presence or absence of furin. As shown in Fig. 1A, RVRR-AmLuc and

RYKR-AmLuc were incubated with furin for one hour at room temperature, and upon the addition of luciferase, both produced an initial burst of bioluminescence resulting from free D-aminoluciferin generated during the incubation with furin, followed by a gradual decrease of the signal over time. At each time point, RVRR-AmLuc produced higher bioluminescent signal than RYKR-AmLuc. In the absence of furin, both bioluminogenic probes generated negligible levels of bioluminescence (for example, at 1 min, for RVRR-AmLuc, 4.5×10^5 R.L.U., which is 3.8% of the signal observed in the presence of furin) demonstrating that both probes are stable and furin-specific (Fig. 1B). The initial signals observed with three probes in the absence of furin are likely due to the trace amounts of D-aminoluciferin still present in the probes even after HPLC purification. This signal decreased with time as the trace D-aminoluciferin was consumed by the luciferase enzyme. At 30 min. after the luciferase addition, the bioluminescent signal of RVRR-AmLuc in the presence of furin was 30-fold higher than that without furin. In contrast, the control probe RRKY-AmLuc generated negligible light emission under identical conditions regardless the presence of furin: 5.8×10^5 R.L.U at 1 min in the presence of furin and 5.6×10^5 R.L.U. in the absence of furin.

Bioluminescence imaging of furin activity in live breast cancer cells

Next, we evaluated the capacity of the probes for detecting furin activity in live cells. It has been established that the majority of human breast cancer cells overexpress furin (16). We confirmed the expression of furin in breast cancer MDA-MB-468Fluc$^+$ cells by fluorescence immunostaining (Fig. 2C), which showed strong furin staining predominantly in the trans-Golgi network, in agreement with previous reports (27). Consequently, we thus used this cell line to evaluate the probes for imaging the furin activity. MDA-MB-468-Fluc$^+$ cells (3×10^5) were imaged at an interval of 5 mins for two hours after the probe addition (2 μM) (Fig. 2A). The signal from each well was quantified as photons/s and plotted as function of time for each probe (Fig. 2B). For both RVRR-AmLuc and RYKR-AmLuc, strong bioluminescent signals were detected, which gradually increased over time and nearly reached a plateau in two hours. In contrast, the control probe showed just the background level of bioluminescence, which increased slightly with two hours. After 60 mins, RRVR-AmLuc generated ~6-fold higher bioluminescence signals in live cells than the control probe. This result correlates with the in vitro data observed with the probes, demonstrating that our probes are cell-permeable and can detect the furin activity in live cells.

To further examine the kinetics of the probes in imaging furin activity in live cells, MDA-MB-468-Fluc$^+$ cells (3×10^5) were imaged for approximately 2h starting immediately after the addition of 2, 10 or 20 μM of RYKR-AmLuc (Fig. 3A & Supporting Information Fig. S6A). The kinetics at 10 and 20 μM shared the same pattern with a fast increase in first 10 mins followed by a slow increase, and the signal intensity was also similar, suggesting that intracellular furin was saturated at 10 μM of the probe (Fig. 3B & Supporting Information Fig. S6B). At 2 μM the bioluminescence signal gradually increased for two hours and as expected, the intensity was lower than that at 10 or 20 μM (Supporting Information Fig. S6B).

Imaging the inhibition of furin activity in live breast cancer cells

To demonstrate that the observed bioluminescent signal can be blocked by the furin inhibitor, we performed the same cell imaging study with RYKR-AmLuc in the presence of the inhibitor Decanoyl-RVKR-CMK (300 μM). The bioluminescence emission decreased significantly; for example, at 30 min., the bioluminescent signal for 20μM of RYKR-AmLuc was 4-fold higher than that in the presence of the furin inhibitor (Fig. 3A&B). This result further confirms that the bioluminogenic probe is specific to furin activity in MBA-MD-468 cells.

Imaging furin activity in living mice

Our in vitro and cell imaging data have indicated that the bioluminogenic probe RVRR-AmLuc produced higher signal than RYKR-AmLuc, thus RVRR-AmLuc was chosen for in vivo imaging of furin activity in tumor xenografts in nude mice. RVRR-AmLuc and the control RRKY-AmLuc were injected via tail vain (100 μL of 10 mM probe in PBS) in the same tumor-bearing mice but two days apart. After injection the animals were imaged every five minutes for 1 hour (Fig. 4A). For RVRR-AmLuc, the signal at the tumor site increased significantly at 10 min, peaked at 25 min, and then decreased slowly within 60 min (Fig. 4B). In contrast, the control probe showed low bioluminescence signals at the tumor site constantly over time (Fig. 4B). The contrast between the two probes on average (n= 4 mice) reached 7.8 folds at 10 min, and 7.6 folds between 25-35 min; at the same time point (25 min), the observed contrast between the two probes was 30-fold in vitro (Fig. 1), and 7.1-fold in cell culture (Fig. 2). Total emission from the tumors (substrates and control) was integrated over one hour for all mice, and on average, the emission for RVRR-AmLuc was 8.7-fold higher than the control RRKY-AmLuc (p=0.017) (Fig. 4C). Histological staining of tumor dissections validated the expected expression of furin (Supporting Information Figure S7). These results demonstrate that our bioluminogenic probes can specifically image furin activity in xenografted breast cancer tumors in mice.

DISCUSSION

Proteases as an important class of enzymes play vital roles in many biological processes such as cell replication, growth, differentiation, viral infection, tumor formation and metastasis, and thus extensive efforts have been made towards developing probes for imaging their activity in vivo (28-30). A generally used method is fluorescence-based by taking advantage of the enzymatic function of cleaving the amide bond between two adjacent amino acid residues to create “smart or activatable” probes through modulation of the fluorescence emission. It can be a specific peptide substrate sequence labeled by a fluorescent emitter at one side of the enzyme cleavage site and a light absorber (or fluorescent acceptor) at the other side of the cleavage site (31,32), or fluorochromes attached to a polymer backbone via a specific peptide substrate (33-35). Due to fluorescence resonance energy transfer or proximity-based self-quenching, these probes emitted little fluorescence before encountering the target proteases, but enhanced fluorescent emission was observed from the proteolytic activity. The similar concept has been applied to the bioluminescence based method for imaging protease activity in vivo (11,12). As shown in this work, it typically involves a conjugate between the substrate of a bioluminescent protein such as firefly luciferase and a synthetic peptide substrate. In comparison to the fluorescence-based in vivo imaging, the bioluminescence imaging offers greater sensitivity (36), although it requires expression of firefly luciferase at the target site.

After the initial demonstration of the commercially available DEVD-aminoluciferin substrate for imaging caspase-3 activity (11,12), there have been few further reports of this method in the literature (13). The bioluminogenic probes we developed here for imaging furin activity represent a latest addition and further demonstrate the value and general applicability of this approach for imaging protease activity in vivo.

We have chosen the tetrapeptidyl substrates of furin over hexapeptidyl substrates even that hexapeptidyl substrates generally display more efficient hydrolytic kinetics because of substrate inhibition observed with hexapeptidyl but not with tetrapeptidyl substrates (37). Between two tetrapeptidyl probes we designed, RVRR-AmLuc showed higher activity than RYKR-AmLuc both in vitro and in vivo. Interestingly, similar substrates Boc-RVRR-MCA (Boc: N-t-butoxycarbonyl; MCA: methylcoumarinamide) have been reported to show less efficient kinetics (k_{cat}/K_m of 3.57×10^3 s^{-1} M^{-1} for furin purified form CHO cells) (25,26)

than Acetyl-RYKR-MCA (k_{cat}/K_m of 5.2×10^5 s^{-1} M^{-1} for human furin) (24), suggesting that the aminoluciferin group may have different effects than the coumarin moiety on the conjugate kinetics.

Furin has a strikingly diverse collection of physiological substrates from growth factors, hormones, receptors and even other proteases, and plays crucial roles in development, homeostasis, and diseases ranging from anthrax, Ebola fever, Alzheimer's disease and cancer(15). Previous fluorogenic substrate Boc-RVRR-MCA is just not useful to non-invasively image furin activity in vivo. Our bioluminogenic probes now fill in the gap and make the in vivo monitoring of furin activity in the same animals in real time feasible.

In summary, we report here "caged" bioluminogenic probes for imaging furin activity in vivo. The probes can be specifically activated by furin and produce bioluminescence emission in the presence of firefly luciferase in vitro, in living breast cancer cells, and in breast cancer tumor xenografts in mice. Non-invasive imaging of furin activity could provide a platform for in vivo assessment of furin-based prodrugs and screening of therapeutic furin inhibitors (19). Moreover, these bioluminogenic probes could allow for investigating the furin role in hypoxia in vivo, and provide a means for in vivo imaging of tumor hypoxia.

Supplementary Material

Refer to Web version on PubMed Central for supplementary material.

Acknowledgments

This work was supported by an IDEA award from Department of Defense Breast Cancer Research Program (W81XWH-09-1-0057) and the NCI's Small Animal Imaging Resource Program (SAIRP R24CA92862). We thank Dr. Contag (Stanford Medical School) for providing MDA-MB-468 $Fluc^+$ cell line.

References

(1). Contag CH, Bachmann MH. Advances in in vivo bioluminescence imaging of gene expression. Annu. Rev. Biomed. Eng 2002;4:235–260. [PubMed: 12117758]

(2). Contag PR, Olomu IN, Stevenson DK, Contag CH. Bioluminescent indicators in living mammals. Nat. Med 1998;4:245–247. [PubMed: 9461201]

(3). Bhaumik S, Gambhir SS. Optical imaging of *Renilla* luciferase reporter gene expression in living mice. Proc. Natl. Acad. Sci. U S A 2002;99:377–382. [PubMed: 11752410]

(4). Drake JM, Gabriel CL, Henry MD. Assessing tumor growth and distribution in a model of prostate cancer metastasis using bioluminescence imaging. Clin. Exp. Metastasis 2005;22:674–684. [PubMed: 16703413]

(5). Rehemtulla A, Stegman LD, Cardozo SJ, Gupta S, Hall DE, Contag CH, Ross BD. Rapid and quantitative assessment of cancer treatment response using in vivo bioluminescence imaging. Neoplasia 2000;2:491–495. [PubMed: 11228541]

(6). Shah K, Jacobs A, Breakefield XO, Weissleder R. Molecular imaging of gene therapy for cancer. Gene Ther 2004;11:1175–1187. [PubMed: 15141158]

(7). Pichler A, Prior J, Piwnica-Worms D. Imaging reversal of multidrug resistance in living mice with bioluminescence: MDR1 P-glycoprotein transports coelenterazine. Proc. Natl. Acad. Sci. U S A 2004;101:1702–1707. [PubMed: 14755051]

(8). De A, Gambhir SS. Noninvasive imaging of protein-protein interactions from live cells and living subjects using bioluminescence resonance energy transfer. FASEB J 2005;19:2017–2019. [PubMed: 16204354]

(9). Luker GD, Sharma V, Pica CM, Dahlheimer JL, Li W, Ochesky J, Ryan CE, Piwnica-Worms H, Piwnica-Worms D. Noninvasive Imaging of Protein-Protein Interactions in Living Animals. Proc. Natl. Acad. Sci. U S A 2002;99:6961–6966. [PubMed: 11997447]

(10). Gross S, Piwnica-Worms D. Spying on cancer: molecular imaging in vivo with genetically encoded reporters. Cancer Cell 2005;7:5–15. [PubMed: 15652745]

(11). Shah K, Tung CH, Breakefield XO, Weissleder R. In vivo imaging of S-TRAIL-mediated tumor regression and apoptosis. Mol. Ther 2005;11:926–931. [PubMed: 15922963]

(12). Liu JJ, Wang W, Dicker DT, El-Deiry WS. Bioluminescent imaging of TRAIL-induced apoptosis through detection of caspase activation following cleavage of DEVD-aminoluciferin. Cancer Biol. Ther 2005;4:885–892. [PubMed: 16177559]

(13). Yao H, So M-K, Rao J. A bioluminogenic substrate for in vivo imaging of beta-lactamase activity. Angew. Chem. Intl. Ed 2007;46:7031–7034.

(14). Bassi DE, Fu J, de Cicco RL, Klein-Szanto AJP. Proprotein convertases: “Master switches” in the regulation of tumor growth and progression. Mol. Carcinogenesis 2005;44:151–161.

(15). Thomas G. Furin at the cutting edge: from protein traffic to embryogenesis and disease. Nat. Rev. Mol. Cell Biol 2002;3:753–766. [PubMed: 12360192]

(16). Cheng M, Watson PH, Paterson JA, Seidah N, Chretien M, Shiu RP. Pro-protein convertase gene expression in human breast cancer. Int. J. Cancer 1997;71:966–971. [PubMed: 9185698]

(17). McMahon S, Grondin F, McDonald PP, Richard DE, Dubois CM. Hypoxia-enhanced expression of the proprotein convertase furin is mediated by hypoxia-inducible factor-1. J. Biol. Chem 2005;280:6561–6569. [PubMed: 15611046]

(18). Bassi DE, De Cicco RL, Mahloogi H, Zucker S, Thomas G, Klein Szanto AJP. Furin inhibition results in absent or decreased invasiveness and tumorigenicity of human cancer cells. Proc. Natl. Acad. Sci. U S A 2001;98:10326–10331. [PubMed: 11517338]

(19). Coppola JM, Bhojani MS, Ross BD, Rehemtulla A. A small-molecule furin inhibitor inhibits cancer cell motility and invasiveness. Neoplasia 2008;10:363–370. [PubMed: 18392131]

(20). Hosaka M, Nagahama M, Kim WS, Watanabe T, Hatsuzawa K, Ikemizu J, Murakami K, Nakayama K. Arg-X-Lys/Arg-Arg motif as a signal for precursor cleavage catalyzed by furin within the constitutive secretory pathway. J. Biol. Chem 1991;266:12127–12130. [PubMed: 1905715]

(21). Henrich S, Cameron A, Bourenkov GP, Kiefersauer R, Huber R, Lindberg I, Bode W, Than ME. The crystal structure of the proprotein processing proteinase furin explains its stringent specificity. Nat. Struct. Biol 2003;10:520–526. [PubMed: 12794637]

(22). White EH, Worther H, Seliger HH, McElroy WD. Amino analogs of firefly luciferase and biological activity thereof. J. Am. Chem. Soc 1966;88:2015–2019.

(23). Shinde R, Perkins J, Contag CH. Luciferin derivatives for enhanced in vitro and in vivo bioluminescence assays. Biochemistry 2006;45:11103–11112. [PubMed: 16964971]

(24). Krysan DJ, Rockwell NC, Fuller RS. Quantitative characterization of furin specificity. J. Biol. Chem 1999;274:23229–23234. [PubMed: 10438496]

(25). Hatsuzawa K, Nagahama M, Takahashi S, Takada K, Murakami K, Nakayama K. Purification and characterization of furin, a Kex2-like processing endoprotease, produced in Chinese hamster ovary cells. J. Biol. Chem 1992;267:16094–16099. [PubMed: 1644796]

(26). Molloy SS, Bresnahan PA, Leppla SH, Klimpel KR, Thomas G. Human furin is a calcium-dependent serine endoprotease that recognizes the sequence Arg-X-X-Arg and efficiently cleaves anthrax toxin protective antigen. J. Biol. Chem 1992;267:16396–16402. [PubMed: 1644824]

(27). Shapiro J, Sciaky N, Lee J, Bosshart H, Angeletti RH, Bonifacino JS. Localization of endogenous furin in cultured cell lines. J. Histochem. Cytochem 1997;45:3–12. [PubMed: 9010463]

(28). Funovics M, Weissleder R, Tung CH. Protease sensors for bioimaging. Anal. Bioanal. Chem 2003;377:956–963. [PubMed: 12955390]

(29). Tung CH. Fluorescent peptide probes for in vivo diagnostic imaging. Biopolymers 2004;76:391–403. [PubMed: 15389488]

(30). Law B, Tung CH. Proteolysis: A biological process adapted in drug delivery, therapy, and imaging. Bioconjugate Chem. March 9;2009 ASAP Online. DOI: 10.1021/bc800500a.

(31). Pham W, Choi Y, Weissleder R, Tung CH. Developing a peptide-based near-infrared molecular probe for protease sensing. Bioconjugate Chem 2004;15:1403–1407.

(32). Lee S, Park K, Lee SY, Ryu JH, Park JW, Ahn HJ, Kwon IC, Youn IC, Kim K, Choi K. Dark quenched matrix metalloproteinase fluorogenic probe for imaging osteoarthritis development in vivo. Bioconjugate Chem 2008;19:1743–1747.

(33). Weissleder R, Tung CH, Mahmood U, Bogdanov A. In vivo imaging of tumors with protease-activated near-infrared fluorescent probes. Nat. Biotechnol 1999;17:375–378. [PubMed: 10207887]

(34). Bremer C, Tung CH, Weissleder R. In vivo molecular target assessment of matrix metalloproteinase inhibition. Nat. Med 2001;7:743–748. [PubMed: 11385514]

(35). Law B, Curino A, Bugge TH, Weissleder R, Tung CH. Design, synthesis, and characterization of urokinase plasminogen-activator-sensitive near-infrared reporter. Chem. Biol 2004;11:99–106. [PubMed: 15112999]

(36). Troy T, Jekic-McMullen D, Sambucetti L, Rice B. Quantitative comparison of the sensitivity of detection of fluorescent and bioluminescent reporters in animal models. Mol. Imaging 2004;3:9–23. [PubMed: 15142408]

(37). Rockwell NC, Krysan DJ, Komiyama T, Fuller RS. Precursor processing by Kex2/furin proteases. Chem. Rev 2002;102:4525–4538. [PubMed: 12475200]

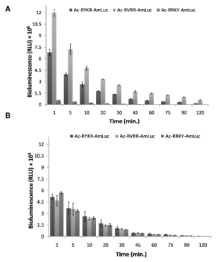

Figure 1.
In vitro detection of furin activity. All substrates were incubated with (*A*) or without 4U (*B*) of furin at room temperature for 1 h. Luciferase buffer and enzyme were added and bioluminescence signal was measured and plotted as the function of time.

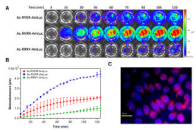

Figure 2.

Furin activity detection in MDA-MB-468Fluc+ cells. *A.* Bioluminescence imaging of cells incubated with Ac-RYKR-AmLuc, Ac-RVRR-AmLuc and Ac-RRKY-AmLuc at 2 μM. *B.* Quantification of the bioluminescence signal; ROIs were drawn over individual wells and the total flux in photon/s was plotted vs. time for each probe. *C.* Furin fluorescence immunostaining of MDA-MB-468 $FLuc^{+}$ cells. Red: furin (Rhodamine-conjugated secondary antibody); blue: nucleus (DAPI).

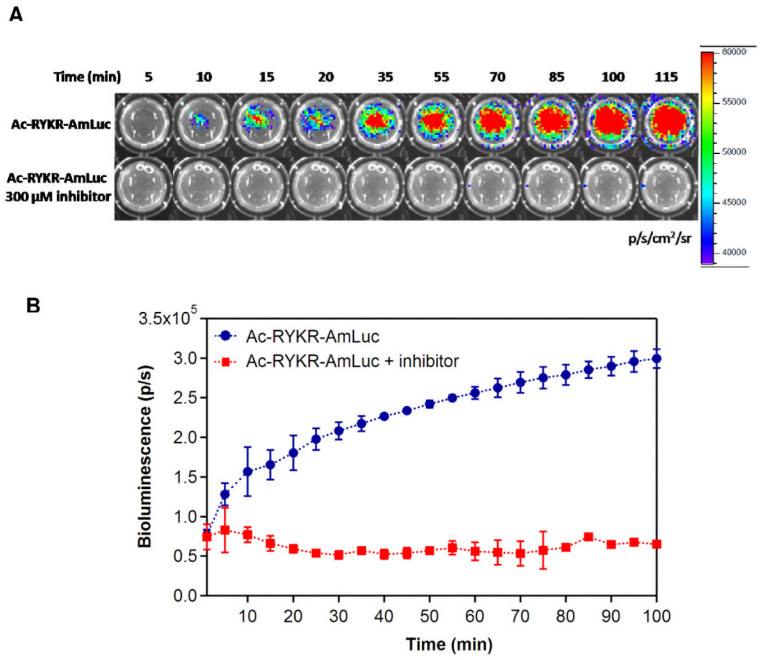

Figure 3.

Imaging the furin inhibition in MDA-MB-468Fluc+ cells. *A*. Bioluminescence imaging of cells incubated with 20 μM of Ac-RYKR-AmLuc in the absence or presence of 300 μM furin inhibitor. *B*. Quantification of the bioluminescence signal; ROIs were drawn over individual wells and the total flux in photon/s was plotted vs. time.

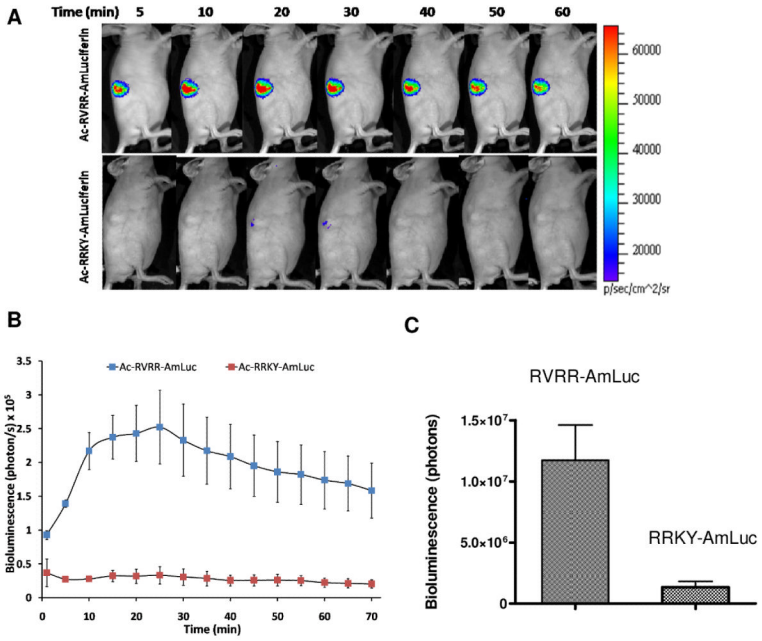

Figure 4.

Bioluminescence imaging of furin activity in xengrafted tumors in nude mice. *A*. Representative bioluminescence imaging of furin activity in the implanted MDA-MB-468Fluc+ cells (n=4). Images were acquired 1 min after tail vain injection of 100 μL (10 mM) of Ac-RVRR-AmLuc (top panel). After two days, the same protocol was applied with injecting Ac-RRKY-AmLuc in the same mice (lower panel). *B*. Quantification of the total flux (photon/s) from the tumor area for Ac-RVRR-AmLuc and negative control, Ac-RRKY-AmLuc. *C*. Integrated bioluminescence emission for mice injected with RVRR-AmLuc and RRKY-AmLuc; p=0.017.

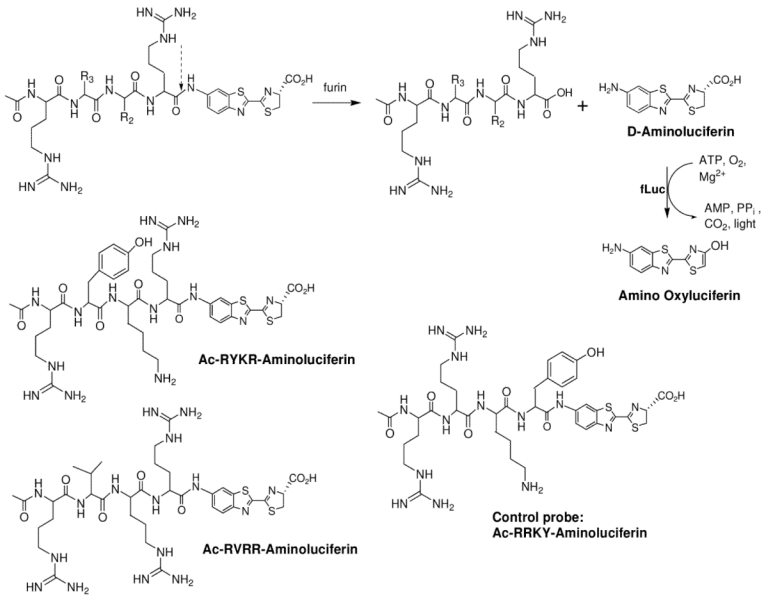

Scheme 1.

Schematic of bioluminogenic probes for detecting furin activity and their chemical structures.